ELSEVIER

Bone 33 (2003) 206–215

BONE

www.elsevier.com/locate/bone

Mathematical model predicts a critical role for osteoclast autocrine regulation in the control of bone remodeling

Svetlana V. Komarova,[a,*] Robert J. Smith,[b] S. Jeffrey Dixon,[a] Stephen M. Sims,[a] and Lindi M. Wahl[b]

[a] *CIHR Group in Skeletal Development and Remodeling, Department of Physiology and Pharmacology and Division of Oral Biology, Faculty of Medicine and Dentistry, University of Western Ontario, London, Ontario, Canada, N6A 5C1*

[b] *Department of Applied Mathematics, University of Western Ontario, London, Ontario, Canada, N6A 5B7*

Received 7 January 2003; revised 26 March 2003; accepted 2 April 2003

Abstract

Bone remodeling occurs asynchronously at multiple sites in the adult skeleton and involves resorption by osteoclasts, followed by formation of new bone by osteoblasts. Disruptions in bone remodeling contribute to the pathogenesis of disorders such as osteoporosis, osteoarthritis, and Paget's disease. Interactions among cells of osteoblast and osteoclast lineages are critical in the regulation of bone remodeling. We constructed a mathematical model of autocrine and paracrine interactions among osteoblasts and osteoclasts that allowed us to calculate cell population dynamics and changes in bone mass at a discrete site of bone remodeling. The model predicted different modes of dynamic behavior: a single remodeling cycle in response to an external stimulus, a series of internally regulated cycles of bone remodeling, or unstable behavior similar to pathological bone remodeling in Paget's disease. Parametric analysis demonstrated that the mode of dynamic behavior in the system depends strongly on the regulation of osteoclasts by autocrine factors, such as transforming growth factor β. Moreover, simulations demonstrated that nonlinear dynamics of the system may explain the differing effects of immunosuppressants on bone remodeling in vitro and in vivo. In conclusion, the mathematical model revealed that interactions among osteoblasts and osteoclasts result in complex, nonlinear system behavior, which cannot be deduced from studies of each cell type alone. The model will be useful in future studies assessing the impact of cytokines, growth factors, and potential therapies on the overall process of remodeling in normal bone and in pathological conditions such as osteoporosis and Paget's disease.

Keywords: Basic multicellular unit; Cyclosporin A; Osteoblast; Paget's disease; Transforming growth factor β; Paracrine

Introduction

Bone remodeling occurs at spatially and temporally discrete sites of the skeleton and involves resorption of existing mineralized tissue by osteoclasts, followed by formation of new bone by osteoblasts [1]. Specific regions of bone are targeted for remodeling due to structural microdefects, thus maintaining the mechanical strength of the skeleton (targeted remodeling) [2,3]. In addition, bone remodeling plays a major role in mineral homeostasis, by providing access to stores of calcium and phosphate [4]. In this case, bone remodeling occurs at random locations, so that every part of the skeleton is remodeled periodically (random remodeling) [2,3]. Disruptions in bone remodeling occur in disorders such as osteoporosis and Paget's disease.

Bone remodeling is a coordinated process involving a team of bone cells working within a structure known as a basic multicellular unit (BMU) [1,5]. The exact signals that lead to initiation of bone remodeling are yet to be defined, although bone lining cells and osteocytes have been implicated in this process [1,6]. On initiation of remodeling, osteoclasts differentiate from their monocytic precursors and resorb bone. Later, osteoblasts differentiate from mesenchymal precursors and form new bone. In a healthy young adult, osteoblasts form the same amount of bone that was

* Corresponding author. Fax: +519-850-2459.
E-mail address: svetlana.komarova@fmd.uwo.ca (S.V. Komarova).

8756-3282/03/$ – see front matter © 2003 Elsevier Science (USA). All rights reserved.
doi:10.1016/S8756-3282(03)00157-1

resorbed by osteoclasts, thus completing the remodeling cycle.

Bone remodeling proceeds simultaneously, but asynchronously at multiple sites that can occupy 5–25% of the bone surface [1]. The progression of bone remodeling at each site is regulated by numerous autocrine and paracrine factors [7,8]. Predicting the cumulative effects of multiple factors on bone remodeling is difficult due to the large number of effectors and the multiple actions attributed to some factors. For example, transforming growth factor β (TGFβ) increases bone formation by a direct action on osteoblast differentiation [9,10]. In addition, TGFβ directly activates osteoclast formation in the absence of osteoblasts, but inhibits osteoclastogenesis in co-cultures of osteoclasts and osteoblasts by decreasing expression of receptor activator of nuclear factor κB ligand (RANKL) on osteoblasts [11]. RANKL and osteoprotegerin (OPG) are critical regulators of bone resorption, that are expressed by osteoblasts and exhibit opposite effects on osteoclasts [12]. Whereas RANKL is a potent stimulator of osteoclasts, OPG prevents the interaction of RANKL with its receptor and inhibits bone resorption [7]. Thus, regulation of bone remodeling is complex, involving the simultaneous actions of a number of factors that affect the formation and/or resorption of bone. Mathematical modeling provides a useful approach to integrate existing knowledge of the regulation of bone cells, and to predict and test possible links between bone formation and resorption.

A theoretical approach to bone biology, known as the mechanostat theory, was formulated by Frost [13], and led to the development of a spectrum of mathematical models depicting the biomechanical properties of bone [14,15]. However, few attempts have been made to mathematically reconstruct the process of bone remodeling at the cellular level. One such model was recently reported, describing the population dynamics of osteoblasts and osteoclasts and focusing on bone remodeling in response to different regimens of parathyroid hormone administration [16].

In the present study, we constructed a mathematical model describing temporal changes in osteoblast and osteoclast populations and consequent changes in bone mass at a single site of bone remodeling. We found that the system can exist in two stable modes: a single remodeling cycle in response to an external stimulus, and a series of internally initiated cycles of bone remodeling. These two modes correspond to targeted and random bone remodeling, respectively. Additionally, a third mode of behavior similar to bone remodeling in Paget's disease was predicted, consisting of unstable oscillatory changes in cell numbers and bone mass with increasing amplitude. Surprisingly, we found that the mode of dynamic behavior of the system depends mainly on the parameter representing autocrine regulation of osteoclasts.

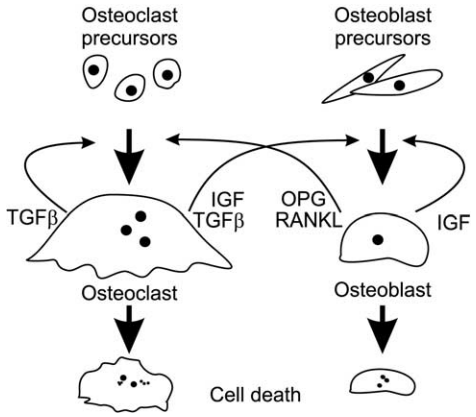

Fig. 1. Schematic representation of interactions between osteoclasts and osteoblasts included in the model. Thick arrows represent the processes of formation and removal of osteoclasts and osteoblasts. Fine arrows represent the effects of autocrine and paracrine regulators of bone remodeling on the rates of osteoclast and osteoblast formation. TGFβ, transforming growth factor β, released and activated by resorbing osteoclasts, directly stimulates formation of osteoclasts and osteoblasts. IGF, insulin-like growth factors, secreted by osteoblasts and released by resorbing osteoclasts, activate osteoblast formation. RANKL, expressed on and released by osteoblasts, activates osteoclastogenesis. OPG, osteoprotegerin, released by osteoblasts, inhibits the actions of RANKL.

Model development

We developed a mathematical model describing the population dynamics of bone cells, with the number of osteoclasts and osteoblasts at a single BMU denoted by x_1 and x_2, respectively (Appendix 1). The rates of overall production of each cell population reflect the net effect of recruitment of precursors and the formation of mature cells. The rates of cell removal reflect cell death, as well as differentiation of osteoblasts into osteocytes and bone lining cells.

We proposed that cells have the ability to interact with each other via effectors, which are released or activated by bone cells and act in an autocrine or paracrine manner (locally affecting the cell type of origin or the other cell type, respectively) (Fig. 1). To summarize the net effect of local factors on the rates of cell production, we employed a power law approximation. Power law approximations were developed by Savageau as effective tools for the analysis of highly nonlinear biochemical systems [17]. This approach is now widely used in exploratory modeling since it adequately describes the nonlinear nature of biological processes, but is sufficiently simple to be used with a wide range of analytical and computational techniques [18,19]. In our model, both osteoclasts and osteoblasts can produce local effectors capable of activating or inhibiting themselves or the other cell type. We made a simplifying assumption that autocrine and paracrine factors regulate only rates of production of osteoclasts and osteoblasts, while the rates of their removal are proportional to the current number of corresponding cells. Although we ignored the fact that some factors, such as RANKL and IGF, can promote osteoclast

and osteoblast survival, this assumption allowed us to decrease the number of parameters, making the model more amenable to comprehensive investigation.

We assumed that the concentration of a particular local effector depends on the number of donor cells at any given time. The parameters g_{ij} described the net effectiveness of autocrine and paracrine factors, reflecting processes such as the amount of effector produced per donor cell and the responsiveness of the target cells. Parameter g_{11} described the combined effects of all factors produced by osteoclasts that regulate osteoclast formation (osteoclast autocrine regulation). Parameter g_{12} described the combined effects of all factors produced by osteoclasts that regulate osteoblast formation (osteoclast-derived paracrine regulation). For example, TGFβ is a factor released and activated by osteoclasts that regulates osteoclast and osteoblast formation. Osteoblast autocrine regulation (g_{22}) included the combined effects of all factors produced by osteoblasts to regulate osteoblast formation. Insulin-like growth factors (IGFs) are examples of factors that are secreted by osteoblasts and can stimulate osteoblast formation [20]. Parameter g_{21} included the combined effects of all factors produced by osteoblasts that regulate osteoclast formation, such as OPG and RANKL (osteoblast-derived paracrine regulation). Initially, we did not limit the model to known interactions; thus no restrictions were imposed on the values of g_{ij}, allowing each cell type to stimulate, inhibit, or have no effect on its own or the other cell type. The following example illustrates the relationship between the parameters of the model and known effectors such as OPG and RANKL. Since both OPG and RANKL are produced by osteoblasts, their concentration is proportional to the number of osteoblasts: [OPG] $\propto x_2$ and [RANKL] $\propto x_2$. Since OPG and RANKL affect osteoclasts, the rate of osteoclast formation in our model is upregulated by the osteoclast activator RANKL, as $\propto$ [RANKL]$^t \propto x_2^t$ and downregulated by the osteoclast inhibitor OPG as $\propto 1/$[OPG]$^s \propto 1/x_2^s$, where t and s reflect the effectiveness of these factors in regulating osteoclast formation. Overall, the rate of osteoclast production depends on the number of osteoblasts as $\propto x_2^{t-s}$, or $x_2^{g_{21}}$, where g_{21} is a parameter describing the effectiveness of osteoblast-derived paracrine regulators, which can be positive or negative depending in this example on the relative activity of RANKL and OPG.

Using these assumptions, we constructed the following system of differential equations to describe the dynamics of cell populations at the bone remodeling site:

$$dx_1/dt = \alpha_1 x_1^{g_{11}} x_2^{g_{21}} - \beta_1 x_1, \tag{1}$$

$$dx_2/dt = \alpha_2 x_1^{g_{12}} x_2^{g_{22}} - \beta_2 x_2, \tag{2}$$

where x_1 and x_2 are the number of osteoclasts and osteoblasts; α_i and β_i are activities of cell production and removal; and parameters g_{ij} represent the net effectiveness of osteoclast- or osteoblast-derived autocrine or paracrine factors.

The third equation in our model describes changes in bone mass. Populations of osteoclasts and osteoblasts under steady-state conditions were assumed to consist of less differentiated cells that were unable to resorb or build bone, but able to participate in autocrine and paracrine signaling. Increases in cell numbers above steady-state levels were attributed to the proliferation and differentiation of precursors into mature cells able to remove or build bone. We assumed that the rates of bone resorption and formation are proportional to the numbers of osteoclasts and osteoblasts (respectively) exceeding steady-state levels:

$$dz/dt = -k_1 y_1 + k_2 y_2, \tag{3}$$

where

$$y_i = \begin{cases} x_i - \bar{x}_i, & \text{if } x_i > \bar{x}_i, \\ 0, & \text{if } x_i \le \bar{x}_i. \end{cases} \tag{4}$$

Here z is total bone mass, k_i is normalized activity of bone resorption and formation, y_i are the numbers of cells actively resorbing or forming bone, and $\bar{x}_i$ are the numbers of cells at steady state.

To estimate the initial parameters of the model, we used experimental data obtained from the histomorphometric analysis of bone sections [1]. It was estimated that initiation of bone resorption in trabecular bone results in differentiation of 10–20 osteoclasts that resorb bone at a rate of 10 μm/day [1,20]. At a single location, maximal erosion is achieved in 9–14 days. Later, about 2000 osteoblasts arrive at the cavity base and build bone at a rate of 1 μm/day [1]. Three to five months after the cycle was initiated, bone returns to a quiescent state (steady state). We used these data to estimate the rate constants of bone cell removal as

$$\beta_1 = 0.2 \text{ day}^{-1}, \tag{5.1}$$

$$\beta_2 = 0.02 \text{ day}^{-1}. \tag{5.2}$$

We chose initial values of g_{ij} that result in behavior similar to that of the bone remodeling cycle:

$$g_{11} = 0.5,\ g_{21} = -0.5, \tag{5.3}$$

$$g_{12} = 1,\ g_{22} = 0. \tag{5.4}$$

We adjusted the rate constants of bone cell formation to obtain reasonable values of steady-state cell numbers at a single remodeling site, in the order of tens for osteoclasts and hundreds for osteoblasts:

$$\alpha_1 = 3 \text{ cells day}^{-1}, \tag{5.5}$$

$$\alpha_2 = 4 \text{ day}^{-1}. \tag{5.6}$$

We present changes in bone mass as relative change from initial value (100%) and chose the constants for normalized activities of bone resorption (k_1) and bone formation (k_2) as follows:

$$k_1 = 0.24\% \text{ cell}^{-1} \text{ day}^{-1}, \tag{5.7}$$

$$k_2 = 0.0017\% \text{ cell}^{-1} \text{ day}^{-1}. \tag{5.8}$$

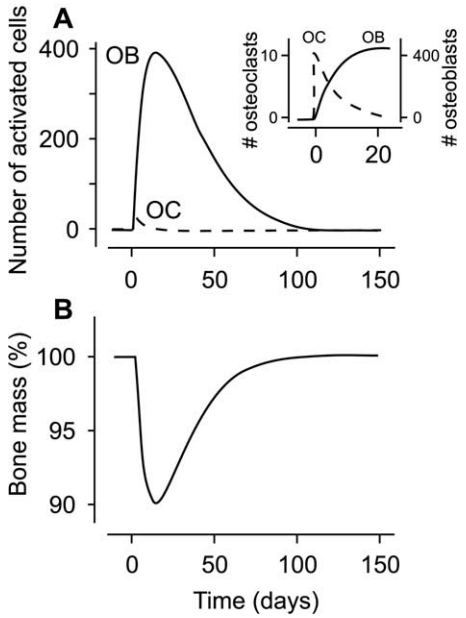

Fig. 2. Simulation of the bone remodeling cycle. (A) Changes with time in the number of osteoclasts (OC, dashed line) and osteoblasts (OB, solid line) calculated from the model. A single event of bone remodeling was initiated by a momentary increase in the number of osteoclasts by 10 cells at time 0. Data are presented as the number of cells exceeding the level before stimulation. Inset: Expanded view of onset of bone remodeling, revealing that an increase in the number of osteoclasts (axis on the left) precedes the increase in the number of osteoblasts (axis on the right). (B) Consequent changes in bone mass are calculated as a percentage of initial bone mass (100%). The pattern of a single remodeling cycle is similar to that observed in vivo and attributed to targeted bone remodeling. Calculations were performed using the following set of parameters. $\alpha_1 = 3$, $\alpha_2 = 4$, $\beta_1 = 0.2$, $\beta_2 = 0.02$, $g_{11} = 0.5$, $g_{12} = 1$, $g_{21} = -0.5$, $g_{22} = 0$, $k_1 = 0.24$, $k_2 = 0.0017$.

We used the initial values of the parameters as a starting point from which we explored the parametric space. We analyzed the stability of steady-state solutions of the system of Eqs. (1) and (2) analytically, and the dynamic behavior of the system of Eqs. (1)–(4) using numerical integration by a fourth-order Runge–Kutta algorithm using Matlab (The Mathworks Inc., 1998) and Berkeley Madonna Version 8.0.1 (R.I. Macey, G.F. Oster, University of California at Berkeley).

Results and discussion

Model predicts different modes of dynamic behavior that resemble targeted and random bone remodeling

First, we examined whether the model simulates the dynamic behavior of the bone remodeling cycle. Bone remodeling was initiated by a momentary increase in the number of osteoclasts at time zero (Fig. 2A). Changes in cell numbers and bone mass were calculated from Eqs. (1)–(4), with initial cell numbers given by the steady-state solution calculated using parameter values described by Eqs. (5). Approximately 20 days after perturbation, osteoclast numbers return to the steady state. While their numbers were elevated, osteoclasts stimulated the slower process of osteoblast formation, leading to an increase in the number of osteoblasts (Fig. 2A). This process is also transient, with osteoblasts slowly returning to basal level after osteoclast removal. Consequent changes in bone mass demonstrate an initial phase of bone resorption followed by a slower phase of bone formation (Fig. 2B), corresponding to a single bone remodeling cycle resembling targeted remodeling in vivo. These data are in good agreement with the temporal pattern of changes in osteoblast and osteoclast populations reconstructed from histomorphometric studies [1].

We systematically investigated the effect of altering parameters on the dynamic behavior of the system, and found that certain parameter values gave rise to stable oscillations of cell numbers and bone mass (Fig. 3). The simulation was started at the steady-state values for the number of osteoclasts and osteoblasts, and, at time zero, bone remodeling was initiated by a momentary increase in the number of osteoclasts. In the case shown in Fig. 3A, the initial perturbation resulted in oscillatory changes in the number of osteoclasts followed by corresponding changes in the number of osteoblasts. The period of oscillations is determined by the rate constants for osteoblast and osteoclast removal and parameters for net autocrine and paracrine regulation [Appendix III, Eq. (A7)].

Consequent changes in bone mass corresponded to a series of remodeling cycles (Fig. 3B). It is important to note

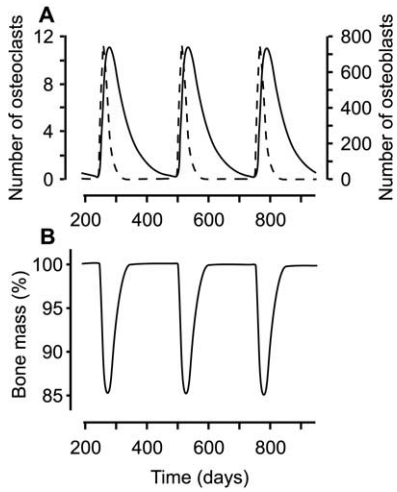

Fig. 3. Stable, intrinsically regulated oscillatory changes in bone cell numbers and bone mass, resembling random bone remodeling. (A) Changes with time in the number of osteoclasts (dashed line, axis on the left) and osteoblasts (solid line, axis on the right) following perturbation by a single increase in the number of osteoclasts by 10 cells at time 0. (B) Consequent changes in bone mass consist of a series of bone remodeling events, each resembling a single remodeling cycle. 100% represents the steady-state level of bone mass. Calculations were performed using the following set of parameters: $\alpha_1 = 3$, $\alpha_2 = 4$, $\beta_1 = 0.2$, $\beta_2 = 0.02$, $g_{11} = 1.1$, $g_{12} = 1$, $g_{21} = -0.5$, $g_{22} = 0$, $k_1 = 0.093$, $k_2 = 0.0008$.

that once these cycles of remodeling had been initiated by a single stimulus, they continued without any external stimuli. Such type of dynamic behavior may represent random bone remodeling. Thus, different types of bone remodeling—targeted and random—could be different modes of dynamic behavior of the same system. It was proposed previously that it would be beneficial in osteoporotic patients to reduce only nontargeted bone remodeling [2]. The model suggests that changes in local autocrine and paracrine factors can determine the type of bone remodeling. Thus, further analysis of the model was performed to identify the factors critical for determining whether bone remodeling proceeds in a targeted or random manner.

Osteoclast autocrine factor regulates the dynamic behavior of the system

We examined the stability and dynamic behavior of the steady-state solution of the system in the space of parameters g_{ij} (Fig. 4). We investigated the stability of the system of differential equations (1) and (2) analytically (Appendixes II and III). Stable behavior in the model included a single response to a perturbation (Fig. 4A, stable nodes, SN), as well as damped and sustained oscillations (Fig. 4A, stable foci, SF). Unstable behavior included oscillation of cell numbers and bone mass with increasing amplitude (Fig. 4A, unstable foci, UF), an infinite increase or decrease to zero in cell numbers, which are biologically irrelevant (Fig. 4A, unstable nodes and saddles, UN and US). The following equations describe the bifurcation surfaces of the system. Surface *A* separates the areas of unstable saddles:

$$(g_{11} - 1)(g_{22} - 1) - g_{12}g_{21} = 0. \quad (6)$$

Surface *B* divides the areas of foci from those of nodes:

$$\left[\frac{\beta_1}{\beta_2}(g_{11} - 1) - (g_{22} - 1)\right]^2 + 4\frac{\beta_1}{\beta_2}g_{12}g_{21} = 0. \quad (7)$$

Surface *C* separates stable and unstable foci and represents the conditions for sustained oscillations:

$$\frac{\beta_1}{\beta_2}(g_{11} - 1) + (g_{22} - 1) = 0. \quad (8)$$

To further investigate the influence of each factor on the stability and type of steady state, we analyzed each parameter g_{11}, g_{22}, g_{12}, and g_{21} separately. Initial parameters (Eqs. 5) were chosen to simulate the behavior of a single remodeling cycle, then single parameters were altered. For each new parameter value, the mode of bone remodeling was identified by analysis of dynamic changes in cell numbers in response to a momentary increase in the number of osteoclasts. Regions displaying similar modes of behavior were plotted as a function of the parameter value (Figs. 4B–E). The requirement for stability of a steady state places limitations on the values that each parameter can take. For osteoblast autocrine regulation, a stable solution with the

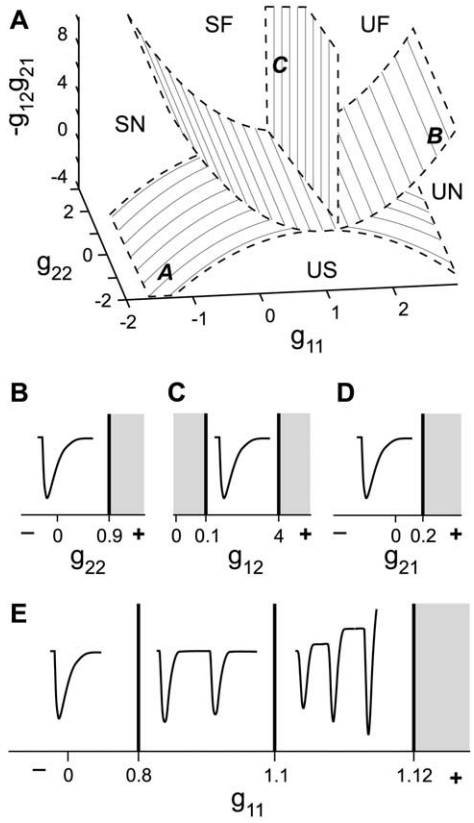

Fig. 4. Osteoclast autocrine regulation g_{11} controls the dynamic behavior of the system. (A) Parametric portrait of the system in the space of parameters g_{11}, g_{22}, $-g_{12}g_{21}$. Bifurcation surfaces (*A, B, C*) are described by Eqs. (6)–(8). The following modes of stable dynamic behavior were observed: stable nodes (SN) and stable foci (SF). Unstable behavior included unstable foci (UF), unstable nodes (UN), and saddles (US). (B–E) The impact of changes in the value of individual parameters on the mode of dynamic behavior. Parameters g_{11}, g_{22}, g_{12}, and g_{21} represent the effectiveness of autocrine and paracrine interactions in the model, which can be negative (inhibitory, −), positive (stimulatory, +), or 0 (no interaction). Initial parameters, Eqs. (5), were chosen to model a single remodeling cycle. Each parameter was gradually altered and bone remodeling was stimulated by a momentary increase in the number of osteoclasts. Changes in the mode of dynamic behavior were monitored and regions demonstrating a similar pattern of behavior were plotted as a function of the parameter, divided by thick border lines. The curves represent the pattern of change in bone mass observed in response to a single stimulation. Shaded areas represent unstable nodes or saddles. (B) Osteoblast autocrine regulation (g_{22}). (C) Osteoclast-derived paracrine regulation (g_{12}). (D) Osteoblast-derived paracrine regulation (g_{21}). (E) Osteoclast autocrine regulation (g_{11}). Under these conditions, changes in the effectiveness of osteoclast autocrine regulation are unique in that they alter the mode of dynamic behavior of the system.

dynamic behavior of a single remodeling cycle exists when g_{22} is less then 0.9 (Fig. 4B). Since IGF is a known positive autocrine regulator of osteoblasts, for the next calculations we assumed g_{22} to be positive but small. A single remodeling cycle is a stable solution for a wide range of positive values for osteoclast-derived paracrine regulation g_{12} (Fig. 4C), reflecting the fact that osteoclast activation leads to an increase in osteoblast formation. Osteoblast-derived paracrine regulation g_{21} is limited to negative or very small

positive values, indicating that the net effect of factors produced by osteoblasts must be inhibitory or neutral for osteoclast formation (Fig. 4D). In this regard, osteoblasts produce two opposite osteoclast regulators, RANKL and OPG. The model suggests that the effects of RANKL do not predominate.

Surprisingly, osteoclast autocrine factor g_{11} demonstrated the ability to switch the system between modes of dynamic behavior (Fig. 4E). Negative or small positive values of g_{11} result in a single remodeling cycle. When g_{11} increases to values between 0.8 and 1.1, the system exhibits damped or sustained oscillations. Further increase in g_{11} results in the development of oscillations with increasing amplitude, and finally the system becomes unstable when g_{11} exceeds 1.12. Thus, under these conditions, osteoclast autocrine regulation is unique in its ability to switch the system between different modes of dynamic behavior.

The model predicts that osteoclast-derived autocrine factors control the dynamic behavior of bone remodeling. One of the limitations of the model is that the parameters describing the effectiveness of autocrine and paracrine regulation do not correspond to a single biological factor, but reflect a combination of processes, such as the amount of effector produced by the donor cell, the receptor density on the target cell, and downstream signaling processes. Interestingly, it was shown recently that TGFβ, which is released from the matrix and activated by resorbing osteoclasts, stimulates osteoclastogenesis [11,22]. Thus, it appears that TGFβ acts as an osteoclast-derived autocrine factor. Further experimental and theoretical studies are required to evaluate the role of osteoclast autocrine regulation in the control of bone remodeling.

Model demonstrates dynamic behavior similar to pathologically accelerated bone remodeling of Paget's disease

The unstable oscillations we describe may be relevant to pathological conditions such as Paget's disease (Fig. 5). Paget's disease is a metabolic bone disorder characterized by accelerated rates of focal bone resorption and formation that result in production of structurally deficient bone [23]. The rates of bone resorption and formation in Pagetic patients increase with the severity of the disease [24]. Under conditions for unstable oscillations in our model, each successive cycle of bone remodeling displays increasing amplitude of changes in the number of osteoclasts and osteoblasts (Fig. 5A). Consequent changes in bone mass demonstrate that resorption increases with each cycle, followed by increased formation (Fig. 5B). With time, the number of osteoblasts required to compensate for accelerated bone resorption is calculated to be on the order of 5000 cells, suggesting that availability of preosteoblasts could limit the rate of bone formation.

To further investigate the spectrum of conditions able to induce unstable oscillations, we analyzed the space in proximity to the bifurcation plane C between the regions of stable and unstable oscillations (Fig. 4A, plane C). This plane is parallel to the $-g_{12}g_{21}$ axis, indicating that changes in these parameters are ineffective in inducing unstable oscillations. We constructed a cross section of plane C in the space of parameters g_{11} and g_{22} (Fig. 5C). Increase in the effectiveness of osteoclast autocrine regulation can bring the system into the region of unstable oscillations (Fig. 5C, arrow from point 1 to point 2). Interestingly, when the system initially exhibits stable oscillations, determined by the value of g_{11}, an increase in the effectiveness of osteoblast autocrine regulation is also able to induce unstable oscillations (Fig. 5C, arrow from point 1 to point 3). Although no alterations in the expression of TGFβ (osteoclast autocrine factor) or IGF (osteoblast autocrine factor) were

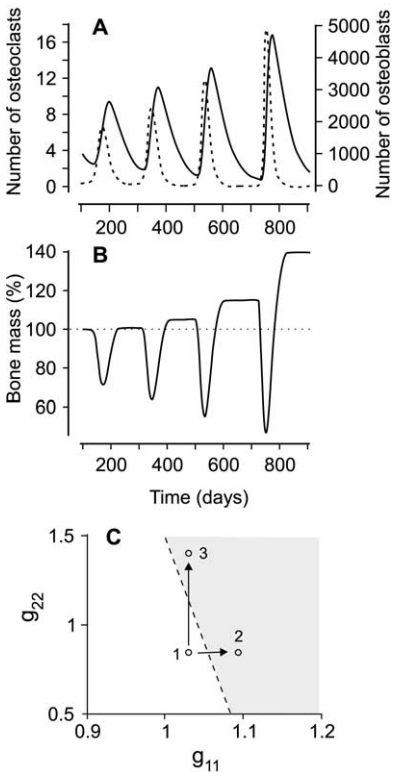

Fig. 5. Unstable oscillations, similar to pathologically accelerated bone remodeling of Paget's disease. (A) Calculated from the model, changes with time in the number of osteoclasts (dashed line) and osteoblasts (solid line) following perturbation by a single increase in the number of osteoclasts by three cells at time 0. (B) Consequent changes in bone mass. 100% (dotted line) indicates bone mass before the perturbation. Unstable (increasing in amplitude) oscillatory changes in bone cell numbers and bone mass are similar to pathologically accelerated bone remodeling of Paget's disease. Calculations were performed using the following set of parameters: $\alpha_1 = 7$, $\alpha_2 = 7$, $\beta_1 = 0.2$, $\beta_2 = 0.02$, $g_{11} = 1.105$, $g_{12} = 1$, $g_{21} = -0.5$, $g_{22} = 0.1$, $k_1 = 0.285$, $k_2 = 0.0008$. (C) Bifurcation line between the regions of stable and unstable oscillations shown in the plane of parameters g_{11}, g_{22}. A small increase in the value of g_{11} (arrow from point 1 to point 2) brings the system into the region of unstable oscillations. Interestingly, when the value of g_{11} is close to the bifurcation line, an increase in g_{22} (arrow from point 1 to point 3) is also able to induce unstable oscillations; however, a larger change in g_{22} is required.

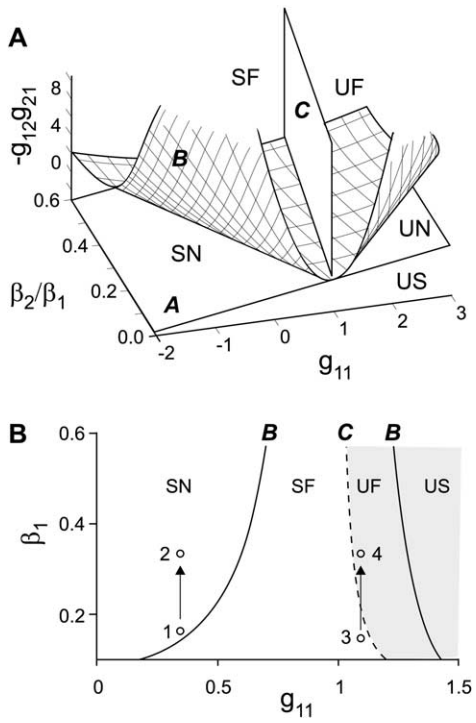

Fig. 6. Effect of rate constant of osteoclast removal on dynamic behavior of the system. (A) Parametric portrait of the system in the space of parameters g_{11}, $-g_{12}g_{21}$, β_2/β_1. Bifurcation surfaces (*A, B, C*) are described by Eqs. (6)–(8). The regions of dynamic behavior include stable nodes (SN), stable foci (SF), unstable foci (UF), unstable nodes (UN), and saddles (US). The vertical plane (*C*) is slightly angled relative to the β_2/β_1 plane, resulting in an area exhibiting paradoxical behavior, further demonstrated in the plane of parameters g_{11} and β_1. (B) The bifurcation lines in the plane of parameters g_{11} and β_1 were calculated assuming other parameters to be $\alpha_1 = 7$, $\alpha_2 = 7$, $\beta_2 = 0.02$, $g_{22} = 0$, $g_{12} = 1$, $g_{21} = -0.5$. Dashed line (*C*) represents the bifurcation line between the regions of stable and unstable oscillations. In contrast to the wide area of parameters (arrow from point 1 to point 2), when the value of g_{11} is close to the bifurcation line (point 3) an an increase in the rate constant of osteoclast removal (β_1) can bring the system into a region of unstable oscillations (arrow from point 3 to point 4).

observed in patients with Paget's disease [25,26], the responsiveness of target cells to these factors was not studied. Alternatively, other osteoclast or osteoblast autocrine activators may be involved.

Rate constants for osteoblast and osteoclast removal affect the dynamic behavior of the system

Since the ratio of the rate constants for osteoclast and osteoblast removal β_1/β_2 affects the stability of the steady state in the model (Eqs. 7 and 8), we investigated its role in controlling the dynamic behavior of the system (Fig. 6). We first developed a three-dimensional parametric portrait of the system based on Eqs. (6)–(8), but now in the space of parameters β_2/β_1, g_{11}, and $-g_{12}g_{21}$ (Fig. 6A, surfaces *A*, *B*, and *C*). The vertical plane *C* is angled slightly with respect to the β_2/β_1 axis, which results in an area exhibiting paradoxical behavior further demonstrated in the space of parameters β_1 and g_{11} (Fig. 6B). Since β_1 represents the rate constant of osteoclast removal, it is natural to expect that an increase in this constant will result in a decrease in a number of osteoclasts and a consequent decrease in the rate of bone resorption (Fig. 6B, arrow from point 1 to point 2). However, in the area adjacent to the bifurcation line (*C*), an increase in β_1 results in the transition of the steady state to the region of unstable oscillations (Fig. 6B, arrow from point 3 to point 4), giving rise to oscillations in cell numbers and bone mass with increasing amplitude. An observer would interpret such behavior as a paradox: an increase in the rate of osteoclast removal results in an increase in bone resorption. Since such discrepancies between the in vitro and in vivo effects of factors regulating bone remodeling were previously reported, we next performed a detailed simulation of this phenomenon.

Interactions between osteoclasts and osteoblasts can give rise to counterintuitive dynamic behavior

We investigated the effects of alteration of the rate constant for osteoclast removal β_1 on the dynamic behavior of a system containing just one variable, the number of osteoclasts (analogous to an in vitro situation). Findings were compared with the effects of a similar alteration in a system that included both osteoclasts and osteoblasts and the full spectrum of interactions between them (analogous to an in vivo situation). To simulate the effect of the increase in β_1 on isolated osteoclasts, we performed calculations using the equation

$$dx_1/dt = \alpha_1 - \beta_1 x_1, \tag{9}$$

where x_1 is the number of osteoclasts, and α_1 is the rate of osteoclast production, assumed to be constant under these conditions. The rate of osteoclast removal is proportional to the number of osteoclasts with rate constant β_1. In this system, an increase in β_1 from 0.20 to 0.23 resulted in a decrease in the number of osteoclasts (Fig. 7A). However, when a similar simulation was performed in the system containing both osteoclasts and osteoblasts (Eqs. 1–4), the result depended on the initial parameters of the system, mainly g_{11} (Figs. 7B,C). First, we chose initial parameters that give rise to a single remodeling cycle ($g_{11} = 0.5$). Remodeling was stimulated before and after the increase in the rate constant of osteoclast removal, β_1 (Fig. 7B). Increase in β_1 led to faster removal of osteoclasts and, consequently, decreased bone resorption and increased steady-state bone mass. The result of the same increase in β_1 is strikingly different when the initial parameters were chosen to give oscillatory dynamic behavior ($g_{11} = 1.109$). In this case, an increase in β_1 led to development of unstable oscillations with increasing amplitude in both cell numbers and bone mass (Fig. 7C). An increase in the number of osteoclasts with each cycle is followed by an increase in the number of osteoblasts, leading to deeper bone resorption

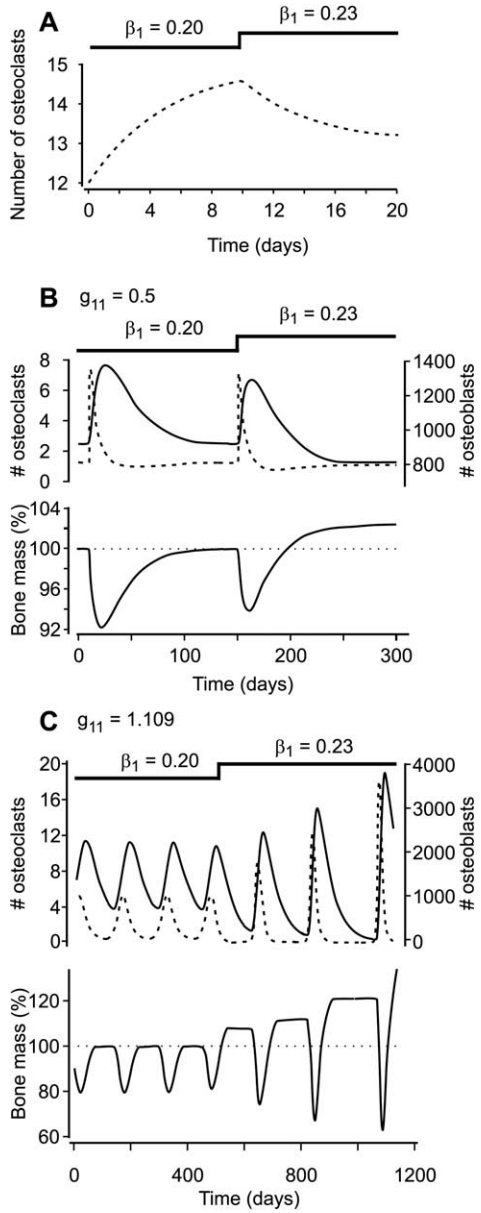

Fig. 7. Simulation of the effects of an increase in the rate constant of osteoclast removal in vitro and in vivo. (A) Changes in the number of osteoclasts (dashed line) in an isolated cell system (in vitro) were calculated using Eq. (9) with $\alpha_1 = 7$ and $\beta_1 = 0.2$. At $t = 10$ days, the rate of osteoclast removal was increased to $\beta_1 = 0.23$, resulting in a decrease in total cell number. (B, C) Changes in the number of osteoclasts (dashed lines), osteoblasts (solid lines), and bone mass in a system that included both osteoclasts and osteoblasts and the full spectrum of interactions between them (in vivo). (B) Effect of an increase in β_1 when the system initially exhibited the dynamic behavior of a single remodeling cycle. Changes with time in the number of osteoclasts and osteoblasts and consequent changes in bone mass (% of initial) were calculated from Eqs. (1)–(4) with initial parameters: $\beta_1 = 0.2$, $g_{11} = 0.5$, $\alpha_1 = 7$, $\alpha_2 = 7$, $\beta_2 = 0.02$, $g_{12} = 1$, $g_{21} = -0.5$, $g_{22} = 0.1$, $k_1 = 0.285$, $k_2 = 0.00057$. Remodeling cycles were initiated by a momentary increase in the number of osteoclasts by seven cells at time $t = 10$ and $t = 150$ days. At $t = 150$ days, the rate of osteoclast removal was increased to $\beta_1 = 0.23$. The increase in osteoclast removal resulted in decreased bone resorption and increased bone mass. (C) Effect of the increase in β_1 on the system initially exhibiting stable oscillatory behavior. Changes with time in the number of osteoclasts and osteoblasts, and consequent changes in bone mass (% of steady state) were calculated from Eqs. (1)–(4) with initial parameters: $\beta_1 = 0.2$, $g_{11} = 1.109$, $\alpha_1 = 7$, $\alpha_2 = 7$, $\beta_2 = 0.02$, $g_{12} = 1$, $g_{21} = -0.5$, $g_{22} = 0.1$, $k_1 = 0.285$, $k_2 = 0.0008$. Remodeling was stimulated by a momentary increase in the number of osteoclasts by three cells at time 0. At $t = 500$ days, the rate of osteoclast removal was increased to $\beta_1 = 0.23$. In this case, the increase in β_1 led to the development of unstable oscillations of cell numbers, resulting in increased bone resorption and enhanced formation.

and enhanced bone formation. However, the number of osteoblasts necessary to compensate for activated bone resorption is in the order of 4000 cells, suggesting that availability of preosteoblasts could be limiting.

Interestingly, the results described above are consistent with experimentally observed effects of immunosuppressants such as cyclosporin A on bone remodeling. Cyclosporin A inhibits osteoclast formation in vitro [27,28]; however, the outcome of treatment with cyclosporin A in vivo appears to depend on the initial state of bone remodeling. Whereas in healthy rats, treatment with cyclosporin A leads to inhibition of bone resorption [29]; in ovariectomized rats, initially presenting with a high turnover state of bone remodeling, the same treatment leads to accelerated bone turnover and osteoporosis [30]. Taken together, the nonlinear dynamics presented in our model may help to explain controversial experimental data regarding the effects of immunosuppressants on bone remodeling. Similarly, the model will be useful in future studies assessing the impact of cytokines, growth factors, and potential therapeutic agents on the overall process of bone remodeling.

Conclusions

We present the first mathematical model to examine the cooperative roles of autocrine and paracrine regulation in the control of bone remodeling. The model is based on the assumption that local effectors produced by osteoclasts and osteoblasts regulate the rates of osteoclast and osteoblast formation. We found that the model predicts different modes of behavior that resemble directed and random bone remodeling and bone remodeling in pathology such as Paget's disease. The system is most sensitive to osteoclast autocrine regulation, reflecting the fact that osteoclasts resorb bone as small teams of very active cells, which are rapidly recruited and then removed. On the other hand, osteoblasts are much less active, and changes in osteoblast numbers occur more slowly; consequently, many more osteoblasts are needed within a single bone remodeling site. The model suggests that, under certain conditions, the availability of preosteoblasts may be a limiting step in the process of bone formation.

To develop this exploratory model, we simplified the complex process of bone remodeling. This strategy resulted in several limitations, including: (1) only two cell types are

considered; (2) only formation of osteoclasts and osteoblasts is regulated by paracrine and autocrine factors, while cellular activity and death are assumed to be proportional to cell number; (3) parameters describing the effectiveness of autocrine and paracrine regulation include the actions of multiple factors; and (4) the power law approximation, a useful tool for model analysis, is not valid when cell numbers approach zero. To address these limitations, more complex models will be required.

In the present study, we demonstrated that, even in a simple form, modeling of the simultaneous processes regulating osteoclasts, osteoblasts, and their interactions results in highly complex, nonlinear behavior. Furthermore, the model indicates that intrinsic properties of the system can give rise to complex modes of bone remodeling observed in vivo.

Acknowledgments

This study was supported by The Arthritis Society, Canadian Arthritis Network, Natural Sciences and Engineering Research Council of Canada, and Canadian Institutes of Health Research. We thank Dr. Beatrice Williams (Department Physiology and Pharmacology, University Western Ontario) and Dr. Victor M. Vitvitsky (National Institute for Hematology, Moscow) for helpful comments on the manuscript. R.J.S. is supported by an Imperial Oil postdoctoral fellowship and L.M.W. holds a Canada Research Chair in Mathematical Biology.

Appendix

I: Nomenclature

α_i	Activities of cell production
β_i	Activities of cell removal
g_{ij}	Effectiveness of the net autocrine or paracrine factors derived from osteoclasts or osteoblasts
g_{11}	Effectiveness of osteoclast autocrine regulation
g_{12}	Effectiveness of osteoclast-derived paracrine regulation
g_{22}	Effectiveness of osteoblast autocrine regulation
g_{21}	Effectiveness of osteoblast-derived paracrine regulation
k_i	Normalized activity of bone resorption and formation
x_1	Number of osteoclasts
x_2	Number of osteoblasts
$\bar{x}_i$	Numbers of cells at steady state
y_i	Numbers of cells actively resorbing or forming bone
z	Total bone mass

II: Steady-state solution

We investigated the stability of the system of differential Eqs. (1) and (2) analytically [17]. The steady-state solutions $(\bar{x}_1, \bar{x}_2)$ were obtained by setting $dx_i/dt = 0$ for $i = 1,2$. A single nontrivial solution in general form is given by the equations

$$\bar{x}_1 = \left(\frac{\beta_1}{\alpha_1}\right)^{(1-g_{22})/\gamma}\left(\frac{\beta_2}{\alpha_2}\right)^{g_{21}/\gamma}, \tag{A1}$$

$$\bar{x}_2 = \left(\frac{\beta_1}{\alpha_1}\right)^{g_{12}/\gamma}\left(\frac{\beta_2}{\alpha_2}\right)^{1-(g_{11}/\gamma)}, \tag{A2}$$

where

$$\gamma = g_{12}g_{21} - (1 - g_{11})(1 - g_{22}). \tag{A3}$$

Trivial solutions exist only when (1) $g_{ij} > 0$ for all i,j; (2) $g_{12} = 0$ and $g_{11} > 0$; and (3) $g_{21} = 0$ and $g_{22} > 0$. Since trivial solutions lie outside the valid range of the power law approximation, the subspace close to zero should be investigated using a different approach.

III: Stability of the steady states

The stability of the nontrivial steady-state solutions in response to small perturbations was investigated analytically following linearization with a Taylor series. The Jacobian of the system is

$$J(\bar{x}_1,\bar{x}_2) = \begin{pmatrix} \alpha_1 g_{11} x_1^{g_{11}-1} x_2^{g_{21}} - \beta_1 & \alpha_1 g_{21} x_1^{g_{11}} x_2^{g_{21}-1} \\ \alpha_2 g_{12} x_1^{g_{12}-1} x_2^{g_{22}} & \alpha_2 g_{22} x_1^{g_{12}} x_2^{g_{22}-1} - \beta_2 \end{pmatrix}. \tag{A4}$$

For the nontrivial solution,

$$J(\bar{x}_1,\bar{x}_2) = \begin{pmatrix} \beta_1(g_{11}-1) & \beta_1 g_{12}\bar{x}_1/\bar{x}_2 \\ \beta_2 g_{21}\bar{x}_2/\bar{x}_1 & \beta_2(g_{22}-1) \end{pmatrix}, \tag{A5}$$

$$\begin{aligned} \operatorname{tr} J(\bar{x}_1,\bar{x}_2) &= \beta_1(g_{11}-1) + \beta_2(g_{22}-1), \\ \det J(\bar{x}_1,\bar{x}_2) &= \beta_1\beta_2(g_{11}-1)(g_{22}-1) \\ &\quad - \beta_1\beta_2 g_{12} g_{21}, \\ \Delta &= \operatorname{tr} J^2 - 4 \det J \\ &= [\beta_1(g_{11}-1) - \beta_2(g_{22}-1)]^2 + 4\beta_1\beta_2 g_{12} g_{21}. \end{aligned} \tag{A6}$$

The nature of the solution depends on the signs of tr $J(\bar{x}_1,\bar{x}_2)$, det $J(\bar{x}_1,\bar{x}_2)$, and Δ. When det $J(\bar{x}_1,\bar{x}_2) = \beta_1\beta_2\,(g_{11} - 1)(g_{22} - 1) - \beta_1\beta_2 g_{12}\, g_{21} < 0$, the solutions are unstable saddles. When tr $J = \beta_1(g_{11} - 1) + \beta_2(g_{22} - 1) > 0$, the solutions are unstable foci or nodes. The condition $\Delta < 0$ divides the areas of foci from those of nodes. The conditions for limit cycles arise on the border surface between damped and unstable oscillations, which are given by the equation $\beta_1\,(g_{11} - 1) + \beta_2\,(g_{22} - 1) = 0$. The solution in this case has the form $x_i = A\,\sin(\Omega t + \phi)$, where the period of oscillations can be calculated as

$$\Omega = 2\pi(\beta_1\beta_2[(1 - g_{11})(1 - g_{22}) - g_{12}g_{21}])^{-0.5}. \quad \text{(A7)}$$

References

[1] Parfitt AM. Osteonal and hemi-osteonal remodeling: the spatial and temporal framework for signal traffic in adult human bone. J Cell Biochem 1994;55:273–86.

[2] Burr DB. Targeted and nontargeted remodeling. Bone 2002;30:2–4.

[3] Parfitt AM. Targeted and nontargeted bone remodeling: relationship to basic multicellular unit origination and progression. Bone 2002; 30:5–7.

[4] Black AJ, Topping J, Durham B, Farquharson RG, Fraser WD. A detailed assessment of alterations in bone turnover, calcium homeostasis, and bone density in normal pregnancy. J Bone Miner Res 2000;15:557–63.

[5] Frost HM. Skeletal structural adaptations to mechanical usage (SATMU): 2. Redefining Wolff's law: the remodeling problem. Anat Rec 1990;226:414–22.

[6] Power J, Loveridge N, Rushton N, Parker M, Reeve J. Osteocyte density in aging subjects is enhanced in bone adjacent to remodeling haversian systems. Bone 2002;30:859–65.

[7] Hofbauer LC, Heufelder AE. Role of receptor activator of nuclear factor-κB ligand and osteoprotegerin in bone cell biology. J Mol Med 2001;79:243–53.

[8] Raisz LG. Physiology and pathophysiology of bone remodeling. Clin Chem 1999;45:1353–8.

[9] Bonewald LF, Dallas SL. Role of active and latent transforming growth factor β in bone formation. J Cell Biochem 1994;55:350–7.

[10] Erlebacher A, Filvaroff EH, Ye JQ, Derynck R. Osteoblastic responses to TGF-β during bone remodeling. Mol Biol Cell 1998;9: 1903–18.

[11] Quinn JM, Itoh K, Udagawa N, Hausler K, Yasuda H, Shima N, et al. Transforming growth factor β affects osteoclast differentiation via direct and indirect actions. J Bone Miner Res 2001;16:1787–94.

[12] Yasuda H, Shima N, Nakagawa N, Yamaguchi K, Kinosaki M, Mochizuki S. Osteoclast differentiation factor is a ligand for osteoprotegerin/osteoclastogenesis-inhibitory factor and is identical to TRANCE/RANKL. Proc Natl Acad Sci USA 1998;95:3597–602.

[13] Frost HM. The mechanostat: a proposed pathogenic mechanism of osteoporoses and the bone mass effects of mechanical and nonmechanical agents. Bone Miner 1987;2:73–85.

[14] Martin B. Mathematical model for repair of fatigue damage and stress fracture in osteonal bone. J Orthop Res 1995;13:309–16.

[15] Turner CH. Toward a mathematical description of bone biology: the principle of cellular accommodation. Calcif Tissue Int 1999;65:466–71.

[16] Kroll MH. Parathyroid hormone temporal effects on bone formation and resorption. Bull Math Biol 2000;62:163–88.

[17] Savageau MA. (Ed.) Biochemical systems analysis: a study of function and design in molecular biology. Reading, MA: Addison–Wesley. Advanced Book Program; 1976.

[18] Ataullakhanov FI, Komarova SV, Vitvitsky VM. A possible role of adenylate metabolism in human erythrocytes: simple mathematical model. J Theor Biol 1996;179:75–86.

[19] Shiraishi F, Savageau MA. The tricarboxylic acid cycle in *Dictyostelium discoideum*. III. Analysis of steady state and dynamic behavior. J Biol Chem 1992;267:22926–33.

[20] Canalis E, Agnusdei D. Insulin-like growth factors and their role in osteoporosis. Calcif Tissue Int 1996;58:133–4.

[21] Jaworski ZF, Duck B, Sekaly G. Kinetics of osteoclasts and their nuclei in evolving secondary haversian systems. J Anat 1981;133: 397–405.

[22] Massey HM, Scopes J, Horton MA, Flanagan AM. Transforming growth factor-β1 stimulates the osteoclast-forming potential of peripheral blood hematopoietic precursors in a lymphocyte-rich microenvironment. Bone 2001;28:577–82.

[23] Noor M, Shoback D. Paget's disease of bone: diagnosis and treatment update. Curr Rheumatol Rep 2000;2:67–73.

[24] Renier JC, Audran M. Polyostotic Paget's disease: a search for lesions of different durations and for new lesions. Rev Rhum Engl Ed 1997;64:233–42.

[25] Mills BG, Frausto A. Cytokines expressed in multinucleated cells: Paget's disease and giant cell tumors versus normal bone. Calcif Tissue Int 1997;61:16–21.

[26] Ralston SH, Hoey SA, Gallacher SJ, Adamson BB, Boyle IT. Cytokine and growth factor expression in Paget's disease: analysis by reverse-transcription/polymerase chain reaction. Br J Rheumatol 1994;33:620–5.

[27] Chowdhury MH, Shen V, Dempster DW. Effects of cyclosporine A on chick osteoclasts in vitro. Calcif Tissue Int 1991;49:275–9.

[28] Orcel P, Denne MA, de Vernejoul MC. Cyclosporin-A in vitro decreases bone resorption, osteoclast formation, and the fusion of cells of the monocyte–macrophage lineage. Endocrinology 1991;128:1638–46.

[29] Orcel P, Bielakoff J, Modrowski D, Miravet L, de Vernejoul MC. Cyclosporin A induces in vivo inhibition of resorption and stimulation of formation in rat bone. J Bone Miner Res 1989;4:387–91.

[30] Movsowitz C, Epstein S, Ismail F, Fallon M, Thomas S. Cyclosporin A in the oophorectomized rat: unexpected severe bone resorption. J Bone Miner Res 1989;4:393–8.